Light-induced oxidative transformation of diphenylamine on ZrO$_2$. Synergism by ZnO and ZnS

CHOCKALINGAM KARUNAKARAN*, SWAMINATHAN KARUTHAPANDIAN**
and PAZHAMALAI VINAYAGAMOORTHY

Department of Chemistry, Annamalai University, Annamalainagar 608002, Tamilnadu, India

Abstract: Diphenylamine (DPA) in ethanol on the surface of ZrO$_2$ undergoes photoinduced oxidative transformation yielding *N*-phenyl-*p*-benzoquinonimine (PBQI). The light-induced transformation on ZrO$_2$ enhanced with DPA concentration, ZrO$_2$-loading, airflow rate and photon flux. The formation of PBQI on ZrO$_2$ is larger on illumination at 254 nm than at 365 nm. The ZrO$_2$ is reusable without any treatment. The mechanism of light-induced oxidative transformation of DPA on ZrO$_2$ is discussed with an appropriate kinetic law. ZnO and ZnS enhance the UV light-induced transformation of DPA on ZrO$_2$, indicating synergism.

Keywords: photooxidation; wide band gap; sub-band gap illumination; photocatalysis.

INTRODUCTION

Semiconductor-photocatalyzed selective organic oxidative transformations have gained interest because of their environmental benign nature and the reviews by Lang *et al.*,[1] Palmisano *et al.*[2] and Shiraishi and Hirai[3] present the different kinds of organic transformations performed photocatalytically. TiO$_2$--based materials are widely used as photocatalysts for organic synthesis.[1–3] Like TiO$_2$, ZrO$_2$ is a nontoxic and photostable IV–VI semiconductor but with a larger band gap energy (≈5 eV). However, this large band gap enables the photocatalytic splitting of water[4] and reduction of CO$_2$.[5,6] The band gap of combustion synthesized ZrO$_2$ is not large (3.5 eV) and Madras and coworkers[7] reported degradation of dyes with illumination at 365 nm; defects in the crystal lattice are the likely reason for the decreased band gap. Here, for the first time, the photoinduced oxidative transformation of diphenylamine (DPA) on untreated ZrO$_2$,

---

which is reusable, is reported. DPA is used in post-harvest treatment of apple and pear[8] and the photosensitized oxidation of DPA is known; cyanoanthracenes[9] and benzophenone[10] are some of the photosensitizers used. The unsensitized photo-oxidation of DPA to N-phenyl-p-benzoquinonimine (PBQI) is slow.[11] The chemical transformation of DPA was studied in the absence and presence of ZrO_2 and the difference in the rates provides the rate of PBQI formation on ZrO_2. The oxidative transformation on ZrO_2 surface was investigated under UV light and under natural sunlight at different experimental conditions to obtain the kinetic law and to elucidate the reaction mechanism. ZnO is a promising II–VI semiconductor photocatalyst with a band gap of 3.2 eV and large excitonic binding energy (60 meV) at room temperature. Although the band gap energy of ZnO is not different from that of TiO_2 and the conduction band (CB) energy levels of the two semiconductors do not differ significantly and so are the valence band (VB) edges, there are reports that ZnO is a better photocatalyst than TiO_2.[12] ZnS is also a II–VI semiconductor but with a wide band gap (≈3.6 eV). Semiconductor mixtures are reported to enhance photocatalytic mineralization of organic molecules[13,14] and here the photoconversion of DPA to PBQI on ZrO_2 was enhanced on mixing ZnO or ZnS with ZrO_2.

EXPERIMENTAL

Materials and measurements

ZrO_2, ZnS and ZnO (Merck) were used as received and their specific surface areas, obtained by BET method, were 15.1, 7.7 and 12.2 m^2 g^{-1}, respectively.[15] The mean particle sizes (t) of ZrO_2, ZnS and ZnO, obtained using the formula $t = 6/\rho S$, where ρ is the material density and S is the specific surface area, are 68, 190 and 87 nm, respectively. The UV–visible diffuse reflectance spectra (DRS) of the semiconductors were obtained using a Shimadzu UV-2600 spectrophotometer with an ISR-2600 integrating sphere attachment. The Kubelka––Munk (KM) plots provide the band gaps of ZnS and ZnO as 3.57 and 3.15 eV, respectively. Potassium tris(oxalato)ferrate(III), $K_3[Fe(C_2O_4)_3]·3H_2O$, was prepared using a standard procedure.[16] DPA, AR (Merck) was used as received. The infrared spectra were recorded on a Nicolet iS5 FT-IR spectrometer. Commercial ethanol was purified by distillation with calcium oxide.

UV light-driven transformation

The UV light-driven transformation on ZrO_2 was performed in a multilamp photoreactor equipped with eight 8 W mercury UV lamps (Sankyo Denki, Japan) emitting at 365 nm. The lamps were shielded by a highly polished anodized aluminum reflector. Four cooling fans mounted at the bottom of the reactor dissipated the generated heat. A borosilicate glass tube of 15-mm inner diameter was used as the reaction vessel and was placed at the center of the photoreactor. The UV light-induced reaction was also studied with a micro-photoreactor fixed with a 6 W 254 nm low-pressure mercury lamp and a 6 W 365 nm mercury lamp. Quartz and borosilicate glass tubes were employed as reaction vessels for 254 and 365 nm lamps, respectively. The light intensity (I) was measured by ferrioxalate actinometry. The volume of the reaction solution was always maintained as 25 mL in the multilamp photoreactor and 10 mL in the micro-photoreactor. Air was bubbled through the solution at a flow rate measured by

the soap bubble method. The UV–Visible spectra were obtained with a Hitachi U-2001 UV––Vis spectrophotometer. The solution was diluted 5-times to lower the absorbance to the Beer–Lambert law limit. The PBQI formed was estimated from its absorbance at 450 nm.

Sunlight-driven transformation

The sunlight-induced transformation on ZrO$_2$ was performed under clear sky in summer (March–July) at 11.30 am–12.30 pm. The solar irradiance (440 W m^{-2}) was measured using a Global pyranometer, supplied by Industrial Meters, Bombay, India. Ethanolic solutions of DPA of the required concentration were prepared afresh and taken in wide cylindrical glass vessels of uniform diameter. The entire bottom of the vessel was covered with ZrO$_2$ powder. Air was bubbled using a micro-pump without disturbing the ZrO$_2$ bed. The volume of DPA solution was 25 mL and the loss of solvent because of evaporation was compensated periodically. The formed PBQI was estimated spectrophotometrically.

RESULTS AND DISCUSSION

UV light-induced oxidative transformation on ZrO$_2$

The UV light-promoted oxidative transformation of DPA in ethanol on ZrO$_2$ surface was realized by bubbling air in a multilamp photoreactor fixed with UV lamps emitting at 365 nm. The UV-visible spectra of the DPA solution recorded at different illumination times show the formation of PBQI (λ_{max} = 450 nm). The time spectra are displayed in Fig. 1. The illuminated solution is EPR silent showing the absence of the formation of diphenylnitroxide. In addition, a thin layer chromatographic experiment revealed the formation of a single product. The illuminated DPA solution was evaporated to dryness after recovery of the particulate ZrO$_2$ and the solid was dissolved in chloroform to develop the chromatogram on a silica gel G-coated plate using benzene as eluent. The PBQI formed was estimated from its absorbance at 450 nm using the reported molar absorptivity.[17,18] The linear increase of the concentration of PBQI with illumination time, as seen in the inset to Fig. 1, provides the PBQI formation rate and the
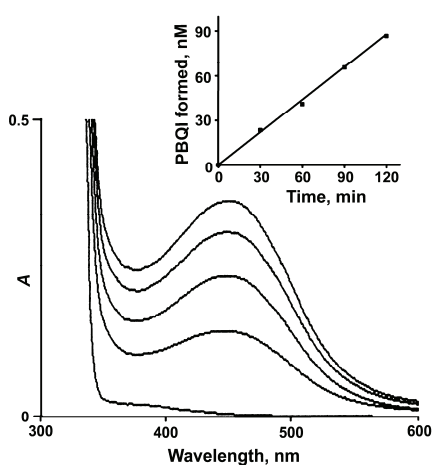

Fig. 1. UV light-induced PBQI formation with ZrO$_2$ in ethanol: the UV-visible spectra of reaction solution (5-times diluted) at 0, 30, 60, 90 and 120 min (increasing A); [DPA] = = 20 mM, ZrO$_2$-loading = 1.0 g, airflow rate = 7.8 mL s^{-1}, I = 13.7×10^{-24} J L^{-1} s^{-1}, volume of reaction solution = 25 mL; inset: Linear increase of formed PBQI with illumination time.

rates were reproducible to ±6 %. The photoformation of PBQI by direct photo-oxidation of DAP in the absence of ZrO_2 was slow[11] and the rate of PBQI formation on ZrO_2 was obtained by measuring the rates of PBQI formation in the presence and absence of ZrO_2. The enhancement of PBQI formation on ZrO_2 with concentration of DPA is displayed in Fig. 2. The observed enhancement conforms to Langmuir–Hinshelwood (LH) kinetics with respect to the DPA concentration. The rate of surface reaction increased with ZrO_2 loading in the DPA solution and the rate reached a limit at a high ZrO_2-loading, as could be seen in Fig. 3. A study of PBQI formation on ZrO_2 as a function of the airflow rate showed enhancement of the surface reaction by oxygen and the rate dependence on the airflow rate conformed to the LH kinetic law, as could be seen in Fig. 4.
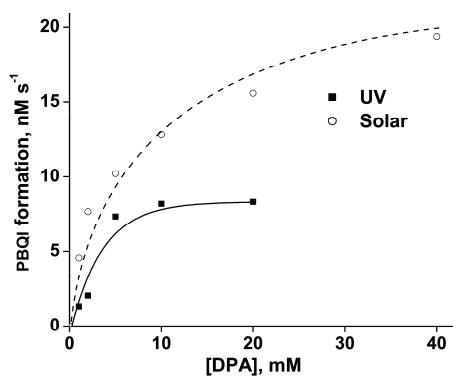

Fig. 2. Light-induced PBQI formation on ZrO_2 as a function of DPA concentration; ZrO_2-loading = 1.0 g, volume of reaction solution = 25 mL; UV: λ = 365 nm, I = = 13.7×10^{-24} J L^{-1} s^{-1}, airflow rate = 7.8 mL s^{-1}; Solar: bed area = 11.36 cm^2, airflow rate = 4.6 mL s^{-1}.
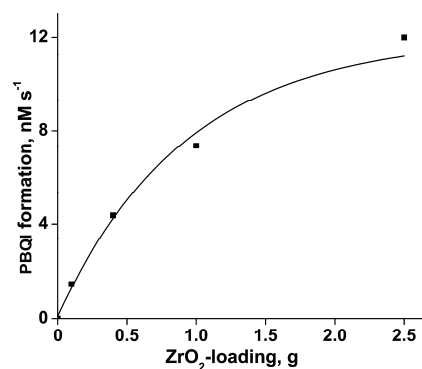

Fig. 3. Photoinduced PBQI formation on ZrO_2 at different ZrO_2-loading; [DPA] = 5.0 mM, airflow rate = 7.8 mL s^{-1}, λ = 365 nm, I = 13.7×10^{-24} J L^{-1} s^{-1}, volume of reaction solution = 25 mL.
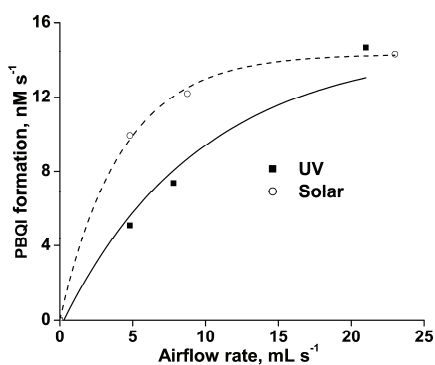

Fig. 4. Photoformation of PBQI on ZrO_2 as a function of airflow rate; [DPA] = 5.0 mM, ZrO_2-loading = 1.0 g, volume of reaction solution = 25 mL; UV: λ = 365 nm, I = 13.7× ×10^{-24} J L^{-1} s^{-1}; solar: bed area = 11.36 cm^2.

The formation of PBQI on ZrO$_2$ was also determined without bubbling air but the solution was not deoxygenated. The dissolved oxygen itself enabled the light-induced surface reaction, but the reaction was slow. PBQI formation on ZrO$_2$ was studied at different intensities of illumination. The chemical transformation was studied with two, four and eight lamps and the angles sustained by adjacent lamps were 180, 90 and 45°, respectively. The dependence of the surface reaction rate on photon flux is displayed in Fig. 5. PBQI was not formed in the absence of illumination. A study of PBQI formation on ZrO$_2$ under UV-A and UV-C light, using a 6 W 365 nm mercury lamp (I = 10.0×10^{-24} J L^{-1} s^{-1}) and a 6 W 254 nm low-pressure mercury lamp (I = 4.09×10^{-24} J L^{-1} s^{-1}), separately in a micro-photoreactor under identical conditions showed that UV-C light was more efficient than UV-A light in inducing the organic transformation on ZrO$_2$. The rate of PBQI formation with UV-A and UV-C light were 9.2 and 20.6 nM s^{-1}, respectively ([DPA] = 5.0 mM, ZrO$_2$ suspended: 1.0 g, airflow rate = = 7.8 mL s^{-1}). The ZrO$_2$ retained its activity on usage. Reuse of ZrO$_2$ showed sustainable light-induced PBQI formation. The azide ion (5 mM), a singlet oxygen quencher, failed to suppress PBQI formation, showing the absence of an involvement of singlet oxygen in the light-induced organic transformation on ZrO$_2$. This finds literature support; Fox and Chen[19] ruled out the possibility of singlet oxygen in the TiO$_2$-photocatalyzed olefin-to-carbonyl oxidative cleavage.
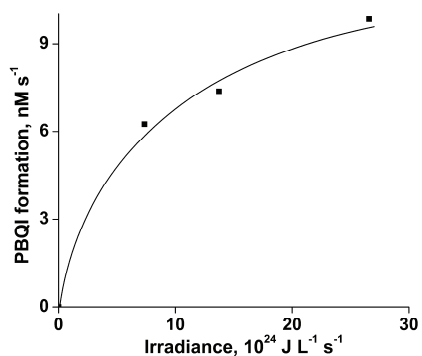

Fig. 5. Influence of photon flux on ZrO$_2$-promoted PBQI formation; [DPA] = 5.0 mM, ZrO$_2$-loading = 1.0 g, airflow rate = 7.8 mL s^{-1}, λ = 365 nm, volume of reaction solution = 25 mL.

Sunlight-induced oxidative transformation on ZrO$_2$

The ZrO$_2$-mediated oxidative transformation of DPA into PBQI also occurs under natural sunlight. The UV–visible spectrum of sun-shined DPA solution in ethanol in the presence of ZrO$_2$ and air was similar to that with UV light (λ_{max} = = 450 nm). Furthermore, the sun-shined solution was EPR silent revealing the absence of diphenylnitroxide. In addition, TLC analysis shows the formation of a single product. Determination of the solar irradiance (W m^{-2}) showed fluctuation of the sunlight intensity during the experiment, even under a clear sky. Hence, the solar experiments under different reaction conditions were performed in a set

to maintain the quantum of sunlight incident on a unit area the same. This enabled comparison of the solar results. A pair of solar experiments performed simultaneously under identical reaction conditions yielded results within ±6 %, which was also the case on different days. The effect of the operational parameters on the solar-promoted oxidative transformation was studied by performing the given set of experiments simultaneously and the results displayed in each figure represent identical solar irradiance. The rate of PBQI formation was obtained by shining the DPA solution on ZrO_2 bed for 60 min. The dependence of PBQI formation rate on the concentration of DPA is shown in Fig. 2. The observed increase of PBQI formation with DPA concentration is characteristic of the LH kinetic law. The double reciprocal plot of the PBQI formation rate *versus* DPA concentration was a straight line with a positive *y*-intercept (figure not shown), which confirmed the LH kinetic model. The rates of PBQI formation on ZrO_2 at different airflow rates are shown in Fig. 4. The observed enhancement of the PBQI formation by oxygen revealed that the surface reaction also conformed to LH kinetics with respect to oxygen. The double reciprocal plot of reaction rate v*ersus* airflow rate was linear with a finite *y*-intercept (figure not presented). The PBQI formation on ZrO_2 was measured without bubbling air but the solution was not deoxygenated. The dissolved oxygen was sufficient to effect the chemical transformation on ZrO_2 during the experimental period. However, the transformation was slow. The PBQI formation on ZrO_2 increased linearly with the apparent area of the ZrO_2-bed, as could be seen in Fig. 6. The oxidative transformation did not occur in the absence of sunlight. ZrO_2 does not lose its activity on usage. Reuse of ZrO_2 showed sustainable activity.
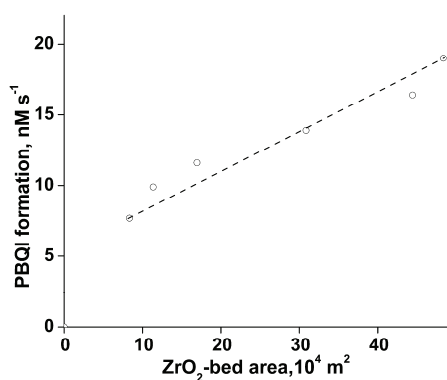

Fig. 6. Dependence of sunlight-driven PBQI formation rate on ZrO_2-bed area; [DPA] = 5.0 mM, ZrO_2-loading = 1.0 g, airflow rate = 4.6 mL s^{-1}, volume of reaction solution = 25 mL.

Mechanism

The DRS of ZrO_2 is presented in Fig. 7, from which it could be observed that the absorption edge of the employed pristine ZrO_2 was 320 nm. Illumination of ZrO_2 with light of wavelength 365 nm is energetically unviable to bring about

band gap excitation and hence the operation of the usual semiconductor-photo-catalysis mechanism is ruled out. DPA is likely to be adsorbed on the surface of ZrO$_2$. The FT-IR spectra of DPA and DPA adsorbed on ZrO$_2$ are displayed in Fig. 8. The shift of the >N–H stretching vibrational frequency from 3408 to 3404 cm^{-1} and bending vibrational frequency from 1595 to 1591 cm^{-1} indicate binding of DPA with ZrO$_2$ through the amine hydrogen. The DRS of DPA-adsorbed ZrO$_2$ shows a shift of the absorption edge to the visible region (413 nm; Fig. 7). This absorption is likely due to electronic excitation of the adsorbed DPA. The excited electron may move to Zr^{4+} resulting in the formation of the radical cation Ph$_2$NH$^{\bullet+}$. The reduced form of Zr^{4+} (*i.e.*, Zr^{3+}) may lose an electron to the adsorbed molecular oxygen yielding superoxide radical ion (O$_2^{\bullet-}$). The reaction of the formed radical cation with the superoxide radical ion may yield the product PBQI.
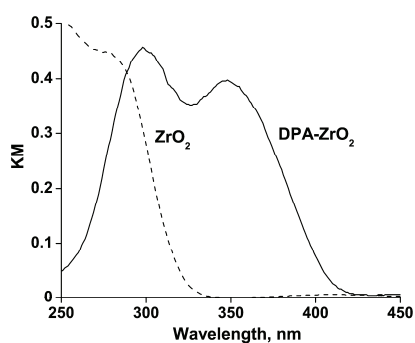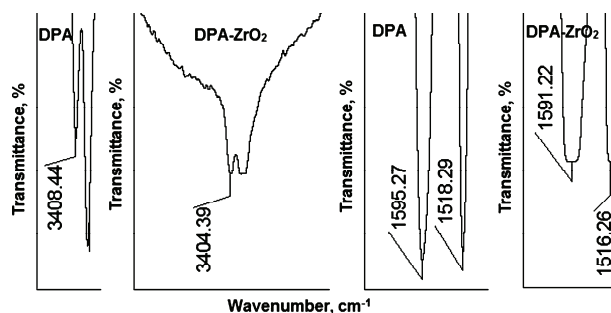

Fig. 7. DRS of bare ZrO$_2$ and DPA-adsorbed ZrO$_2$.

Fig. 8. FT-IR spectra of DPA and DPA-adsorbed ZrO$_2$.

Ali *et al.*[20] studied the photodegradation of methylene blue on ZnO films, deposited on glass slides by either the hydrothermal method or the magnetron sputtering technique, with UV-C light and the results conformed to the LH kinetic law. Leaching of zinc due to photocatalysis was reported under oxygen limited conditions but the ZnO films were observed to be more stable under oxygen-rich conditions. It was suggested that the oxygen from the ZnO lattice

was removed and used in the radical initiation and propagation phases of the photocatalysis under oxygen-limited conditions. That is, the observed deformation of the ZnO lattice over time was ascribed to the use of lattice oxygen in the photocatalytic process. Oxygen-rich conditions either minimize the release of or replace the last ZnO lattice oxygen and the authors proposed the operation of a Mars Van Krevelen (MVK) type mechanism in the photocatalytic degradation of methylene blue under oxygen-limited conditions. In a similar study with UV-A and UV-C light, the same authors suggested the predominance of the MVK mechanism under UV-C illumination.[21] However, Delmon[22] stated that the re-oxidation step in the MVK mechanism is often too slow and consequently the catalysts become reduced in the corresponding reduction–oxidation cycle. That is, the photocatalytic activity is decreased remarkably on reuse. Furthermore, irrespective of the operative mechanism, leaching of zinc or a small decrease in the photocatalytic activity of ZnO on repeated reuse is well known.[23,24] However, ZrO_2 is chemically unreactive and hence operation of a MVK type mechanism in the present study is unlikely. In addition, the fact that ZrO_2 shows sustainable photocatalytic activity (PBQI formation rate was not lowered on reuse of ZrO_2) does not support the operation of a MVK type mechanism in the title reaction. Serpone and co-workers[25–28] stated that both the LH and Eley–Rideal (ER) models are applicable for semiconductor photocatalytic reactions. The LH model presents the adsorption of both the reactant molecules on the surface[29] while the ER model represents adsorption of one of the reactants on the surface; the other reactant molecule interacts with adsorbed reactant molecule to form the product. The LH model requires saturation kinetics with respect to both the reactants whereas the ER model demands saturation kinetics with respect to one of the reactants and first order dependence of the reaction rate with respect to the other reactant. The studied photocatalyzed reaction on ZrO_2 surface shows saturation kinetics with respect to DPA as well as oxygen (Figs. 2 and 4) and hence operation of the ER reaction mechanism is ruled out. Although Bansal and Sidhu[30] stated that singlet oxygen is the oxidant in dye-sensitized photooxidation of DPA, this has been ruled out in the present photocatalytic transformation as azide ion does not suppress the formation of PBQI (*vide supra*); de Lasa *et al.*[31] also proposed the formation of reactive species superoxide radical anion in semiconductor photocatalyzed reactions.

Kinetic law

The heterogeneous photoinduced reaction occurring in a continuously stirred tank reactor (CSTR) conforms to the kinetic law:[32]

$$\text{Rate of PBQI formation on } ZrO_2 = \frac{kK_1K_2SIC[\text{DPA}]\gamma}{(1+K_1[\text{DPA}])\cdot(1+K_2\gamma)} \quad (1)$$

where K_1 and K_2 are the adsorption coefficients of DPA and O_2 on the illuminated ZrO_2 surface, k is the specific rate of oxidation of DPA on the ZrO_2 surface, γ is the airflow rate, S is the specific surface area of ZrO_2, C is the amount of ZrO_2 suspended per liter and I is the light intensity. The data-fit to the LH kinetic curve, drawn using a computer program,[32] confirmed the kinetic law (Figs. 2 and 4). The linear double reciprocal plots of surface reaction rate *versus* the DPA concentration and the airflow rate supports the LH kinetic law. The data-fit provides the adsorption coefficients K_1 and K_2 as 76 L mol^{-1} and 0.039 mL^{-1} s, respectively, and the specific reaction rate k as 2.75×10^9 mol L m^{-2} J^{-1}. However, the rate of PBQI formation on ZrO_2 surface fails to increase linearly with ZrO_2-loading. This is because of the high ZrO_2 loading. At high ZrO_2 loadings, the surface area of the ZrO_2 exposed to illumination does not correspond to the weight of ZrO_2. The quantity of ZrO_2 used is beyond the critical amount corresponding to the volume of the reaction solution and reaction vessel; the whole quantity of ZrO_2 is not exposed to light. The photoinduced transformation lacks linear dependence on the illumination intensity; a lower than first power dependence of a surface-photoreaction rate on the light intensity at high photon flux is well known.[33]

Synergism by ZnO and ZnS

Vectorial transfer of electrons and holes from one semiconductor to another is possible in semiconductor mixtures under band gap-illumination. This charge separation enhances the photocatalytic activity.[13,14] However, what was observed in this study was enhanced phototransformation due to the presence of the semiconductor ZnO or ZnS nanoparticles with ZrO_2 nanoparticles; the wavelength of illumination could effect the band gap excitation of ZnO and ZnS but not ZrO_2. The enhanced formation of PBQI with ZrO_2 mixed with ZnO or ZnS is displayed in Fig. 9; the two nanoparticles were kept under suspension and under continuous motion by bubbling air through the illuminated solution. Aggregation of nanoparticles under suspension is known.[34] The particle size distribution of ZrO_2, ZnO and ZnS under suspension, determined by the light scattering method, are presented in Fig. 10. Examination of Fig. 10 along with the size of the particles obtained from the XRD and BET methods revealed aggregation of the nanoparticles. As observed in the individual ZrO_2, ZnO and ZnS suspensions, aggregation in the ZrO_2–ZnO and ZrO_2–ZnS mixtures under suspension is likely, and both ZrO_2 and ZnO or ZnS nanoparticles are likely to be present in the aggregate. This may lead to transfer of the generated hole from the illuminated ZnO or ZnS to the DPA molecule adsorbed on ZrO_2 surface, resulting in enhanced photooxidation. The densities and particle sizes of ZrO_2, ZnO and ZnS are different and this may be a reason for not observing maximum enhanced photo-oxidation at 50 % composition.
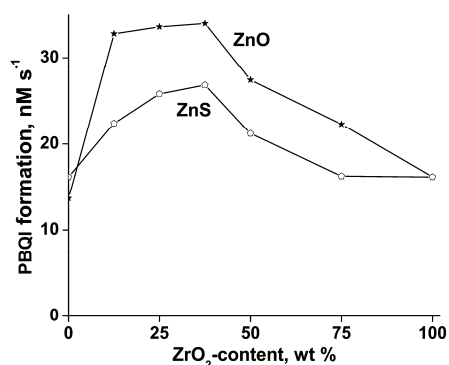
Fig. 9. Enhanced PBQI formation on mixing ZrO_2 with ZnO or ZnS; [DPA] = 5.0 mM, nanoparticles-loading = 1.0 g, airflow rate = 7.8 mL s^{-1}, λ = 365 nm, I = 13.7×10^{-24} J L^{-1} s^{-1}, illumination time = 30 min, volume of reaction solution = 25 mL.
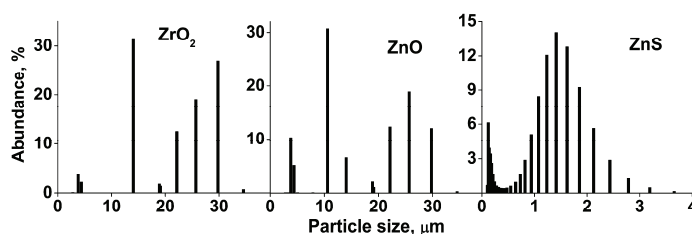

Fig. 10. Particles aggregation.

CONCLUSIONS

ZrO_2 mediates photoinduced oxidative transformation of DPA to PBQI. The formation of PBQI on ZrO_2 enhances with DPA concentration, airflow rate and photon flux and conforms to the Langmuir–Hinshelwood kinetic law. The PBQI formation on ZrO_2 is greater with UV-C light than with UV-A light. ZrO_2 mixed with ZnO or ZnS affords more PBQI than the individual nanoparticles due to synergism.

И З В О Д
ФОТО-ИНДУКОВАНА ОКСИДАТИВНА ТРАНСФОРМАЦИЈА ДИФЕНИЛАМИНА НА ZrO₂. СИНЕРГИЗАМ ZnO И ZnS

C. KARUNAKARAN, S. KARUTHAPANDIAN и P. VINAYAGAMOORTHY

Department of Chemistry, Annamalai University, Annamalainagar 608002, Tamilnadu, India

Дифениламин (DPA) у етанолу на површини ZrO_2 подлеже фото-индукованој оксидативној трансформацији дајући *N*-фенил-*p*-бензохинонимин (PBQI). Фото-индукована трансформација на ZrO_2 се повећава са порастом [DPA], количине ZrO_2, брзине протока ваздуха и флукса фотона. Стварање PBQI на ZrO_2 је веће при озрачивању на 254 nm него на 365 nm. ZrO_2 се може поново користити без икаквог третмана. Механизам фото-индуковане оксидативне трансформације DPA на ZrO_2 је разматран применом одгова-

рајућег кинетичког закона. ZnO и ZnS повећавају UV фото-индуковану трансформацију DPA на ZrO$_2$ указујући на синергизам.

REFERENCES

1. X. Lang, X. Chen, J. Zhao, *Chem. Soc. Rev.* **43** (2014) 473
2. G. Palmisano, E. Garcia-Lopez, G. Marci, V. Loddo, S. Yurdakal, V. Augugliaro, L. Palmisano, *Chem. Commun.* **46** (2010) 7074
3. Y. Shiraishi, T. Hirai, *J. Photochem. Photobiol., C* **9** (2008) 157
4. M. J. Poston, A. B. Aleksandrov, D. E. Sabo, Z. J. Zhang, T. M. Orlando, *J. Phys. Chem., C* **118** (2014) 12789
5. S. Yoshida, Y. Kohno, *Catal. Surv. Jpn.* **4** (2000) 107
6. Y. Kohno, T. Tanaka, T. Funabiki, S. Yoshida, *Chem. Commun.* (1997) 841
7. S. Polisetti, P. A. Deshpande, G. Madras, *Ind. Eng. Chem. Res.* **50** (2011) 12915
8. A. Zanella, *Postharvest Biol. Technol.* **27** (2003) 69
9. Y. C. Chang, P. W. Chang, C. M. Wang, *J. Phys. Chem., B* **107** (2003) 1628
10. T. S. Lin, J. Retsky, *J. Phys. Chem.* **90** (1986) 2687
11. C. Karunakaran, S. Karuthapandian, *Sol. Energy Mater. Sol. Cells* **90** (2006) 1928
12. Y. Li, W. Xie, X. Hu, G. Shen, X. Zhou, Y. Xiang, X. Zhao, P. Fang, *Langmuir* **26** (2010) 591
13. C. Karunakaran, R. Dhanalakshmi, P. Gomathisankar, *Int. J. Chem. Kinet.* **41** (2009) 716
14. C. Karunakaran, R. Dhanalakshmi, P. Gomathisankar, G. Manikandan, *J. Hazard. Mater.* **176** (2010) 799
15. C. Karunakaran, R. Dhanalakshmi, P. Gomathisankar, *Spectrochim. Acta A* **92** (2012) 201
16. D. M. Adams, J. B. Raynor, *Advanced Practical Inorganic Chemistry*, Wiley, New York, USA, 1965, p. 54
17. S. Puri, W. R. Bansal, K. S. Sidhu, *Indian J. Chem.* **11** (1973) 828
18. W. R. Bansal, N. Ram, K. S. Sidhu, *Indian J. Chem., B* **14** (1976) 123
19. M. A. Fox, C. C. Chen, *J. Am. Chem. Soc.* **103** (1981) 6757
20. A. M. Ali, E. A. C. Emanuelsson, D. A. Patterson, *Appl. Catal., B* **91** (2010) 168
21. A. M. Ali, E. A. C. Emanuelsson, D. A. Patterson, *Appl. Catal., B* **106** (2011) 323
22. B. Delmon, *Catal. Today* **117** (2006) 69
23. W. Xie, Y. Li, W. Sun, J. Huang, H. Xie, X. Zhao, *J. Photochem. Photobiol., A* **216** (2010) 149
24. C. Karunakaran, P. Vinayagamoorthy, J. Jayabharathi, *Langmuir* **30** (2014) 15031
25. A. V. Emeline, V. K. Ryabchuk, N. Serpone, *Catal. Today* **122** (2007) 91
26. N. Serpone, A. Salinaro, A. Emeline, V. Ryabchuk, *J. Photochem. Photobiol., A* **130** (2000) 83
27. A. V. Emeline, V. Ryabchuk, N. Serpone, *J. Photochem. Photobiol., A* **133** (2000) 89
28. S. E. Braslavsky, A. M. Braun, A. E. Cassano, A. V. Emeline, M. I. Litter, L. Palmisano, V. N. Parmon, N. Serpone, *Pure Appl. Chem.* **83** (2011) 931
29. V. K. Sharma, C. R. Burnett, W. Rivera, V. N. Joshi, *Langmuir* **17** (2001) 4598
30. W. R. Bansal, K. S. Sidhu, *J. Photochem.* **5** (1976) 156
31. H. de Lasa, B. Serrano, M. Salaices, *Photocatalytic Reaction Engineering*, Springer, New York, 2005, p. 2
32. C. Karunakaran, S. Senthilvelan, *Curr. Sci.* **88** (2005) 962
33. L. Vincze, T. J. Kemp, *J. Photochem. Photobiol., A* **87** (1995) 257
34. M. Li, M. E. Noriega-Trevino, N. Nino-Martinez, C. Marambio-Jones, J. Wang, R. Damoiseause, F. Ruiz, E. M. V. Hock, *Environ. Sci. Technol.* **45 (**2011) 8989.